Notable efficacy of co-treatment with FHD-286, a dual BRG1/BRM ATPase inhibitor, and Menin or BET inhibitor, decitabine or venetoclax against AML with MLLr or mutant NPM1

Warren Fiskus[1], Jessica Piel[2], Murphy Hentemann[2], Christopher P. Mill[1], Christine E. Birdwell[1], Kaberi Das[1], John A. Davis[1], Hanxi Hou[1], Noor Alhamadani[1], Kevin Philip[1], Alicia Matthews[1], Tapan M. Kadia[1], Naval Daver[1], Sanam Loghavi[1], Branko Cuglievan[1], Courtney D. DiNardo[1], and Kapil N. Bhalla[1].

[1]The University of Texas MD Anderson Cancer Center, Houston, TX; [2] Foghorn Therapeutics, Cambridge, MA

THE UNIVERSITY OF TEXAS MD Anderson Cancer Center — Making Cancer History®

Poster Session Online

American Society of Hematology — Helping hematologists conquer blood diseases worldwide

604. Molecular Pharmacology and Drug Resistance: Myeloid Neoplasms: Poster III

Warren Fiskus

MON-4160

ASH2023

Introduction

DNA in eukaryotic cells is packaged in nucleosomes and higher order chromatin structures, making it relatively inaccessible to transcriptional machinery. ATP-dependent chromatin-modifying and remodeling complexes allow transcriptional machinery, composed of transcription factors (TFs) and co-factors, to gain access and modulate transcription. Chromatin remodeling complexes, e.g., BAF complex, contain one ATPase, BRG1 (SMARCA4) or BRM (SMARCA2), and several other factors. The BAF (BRG1/BRM-associated factor) complex is essential for lineage specific gene expression by TFs and for hematopoiesis. Expression and dependency on BRG1/BRM have also been documented for AML cells. Mutations in BRG1 and other BAF complex components are common and mechanistically involved in various cancer types. Recently, cancer cells with mutation and reduced expression of BRG1 were shown to be dependent for survival on the BRM activity of the BAF complex. BRM depletion was shown to selectively inhibit in vitro and in vivo growth of BRG1 mutant cancer cells. BRG1 and BRM have high protein sequence homology, and both contain the core catalytic ATPase domain that drives chromatin remodeling. BRG1 and BRM also contain a bromodomain, which is not a dependency in cancer cells. Small molecule inhibitors of dual BRM and BRG ATPase activity have been developed, which repress BRG1/BRM-dependent gene-expression and growth of cancer cells. FHD286 (Foghorn Therapeutics) is a highly potent, selective, small molecule, oral, catalytic enzyme activity inhibitor of BRM and BRG1. FHD286 is active against AML cells. Evaluation of the CRISPR-dependency screen map (DepMap) showed greater dependency of numerous AML cell lines on SMARCA4 expression. FHD-286 is currently being evaluated in AML for clinical efficacy in early clinical trials.* However, it is unclear which of the genetically characterized AML sub-types, including those associated with poor clinical outcome, would be susceptible or resistant to FHD286. Gene expression signature (GES) of FHD286 activity also needs to be elucidated and tested. In the present studies, we interrogated the in vitro and in vivo efficacy of FHD-286 in inducing differentiation and loss of viability, as well as their molecular correlates in AML cell lines and patient-derived (PD) AML cells. Exposure to FHD-286 overcame differentiation block and significantly induced CD11b expression and morphologic features of differentiation in AML cell lines with MLL-r or mtNPM1. This was followed by a loss of viability of the differentiated AML cells. FHD-286 treatment also induced significant loss of viability in PD AML cells. Following treatment FHD-286, RNA-Seq analysis of MOLM13 cells demonstrated significant reduction in the normalized enrichment scores for expressions of gene-sets of targets of MYC, mTORC1, E2F, Interferon-gamma, IL6-JAK-STAT3, inflammatory response and oxidative phosphorylation genes. QPCR analyses determined significant reduction in mRNA expression of MYC, SPI1 and BCL2 genes. Western analyses showed that treatment with FHD-286 significantly increased p21, p27, PU.1 and CD11b expressions, while reducing expressions of c-Myc and BCL2. Based on these observations, and clinical efficacy of the combination of venetoclax and decitabine/azacitidine, we determined in vitro lethal activity of co-treatment with FHD-286 and venetoclax or decitabine against AML cell lines and PD AML cells. Notably, co-treatment with FHD-286 and venetoclax or decitabine exerted synergistic lethality against AML cell lines and PD AML cells, especially those expressing MLL-r, mtNPM1 or EVI1. Based on the known efficacy of the Menin inhibitor SNDX-50469 in AML with MLL-r or mtNPM1, we also found that co-treatment with FHD-286 and SNDX-50469 was synergistically lethal against AML cell lines and PD AML cells with MLL-r or mtNPM1. Since treatment with BET (bromodomain and extraterminal) protein inhibitor also inhibits c-Myc and BCL2 expression and was shown to be lethally active in AML cells with MLL-r or mtNPM1, we also found that co-treatment with FHD-286 and BET protein inhibitor OTX015 exerted synergistic lethality against AML cell lines and PD AML cells with MLL-r or mtNPM1. We also determined that ex vivo and in vivo treatment with FHD-286 attenuated AML initiating stem cells in PDX models with mtNPM1 and FLT3-ITD. Finally, in luciferase-transduced, patient-derived xenograft (PDX) models of AML cells with MLL-AF9 and FLT3, or mtNPM1 and FLT3-ITD, we determined that treatment with FHD-286 administered orally alone was significantly effective in reducing AML burden and improving overall survival of the mice. Additionally, co-treatment with FHD-286 and venetoclax, decitabine, OTX015 or Menin inhibitor SNDX-5613, as compared to each drug alone or vehicle control, significantly reduced the AML burden and improved median and overall survival of the NSG mice, without inducing significant toxicity. Taken together, these findings highlight the promise of FHD-286 treatment alone and in rational combinations in exerting significant anti-AML efficacy against cellular models of AML, especially those with MLL-r, mtNPM1 or chromosome 3q26 lesions and EVI1 overexpression.

*** Please visit https://foghorntx.com/ for current clinical status.**

Results

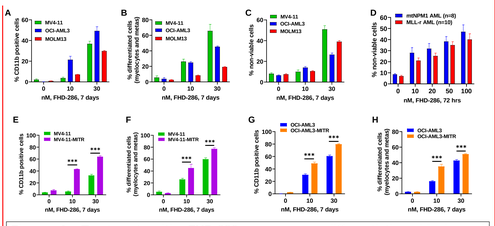

Figure 1. Treatment with FHD-286 overcomes differentiation block and significantly induced CD11b expression and morphologic features of differentiation in AML cell lines with MLL1r and mtNPM1. A-C. MV4-11, OCI-AML3 and MOLM13 cells were treated with the indicated concentrations of FHD-286 for 7 days. At the end of treatment, cells were assessed for CD11b expression, morphologic features of differentiation and percentage of non-viable cells. Columns, mean of three experiments, Bars, S.E.M. **D**. Patient-derived (PD) mtNPM1 and MLL1-r AML cells were treated with the indicated concentrations of FHD-286 for 72 hours. Following this, cells were stained with TO-PRO-3 iodide and the % non-viable cells were determined by flow cytometry. **E-H**. MV4-11, MV4-11-MITR, OCI-AML3 and OCI-AML3-MITR cells were treated with the indicated concentrations of FHD-286 for 7 days. Following this, cells were assessed for the % expression and the mean fluorescent intensity (MFI) of CD11b by flow cytometry and morphologic features of differentiation. Columns, mean of three experiments, Bars, S.E.M.

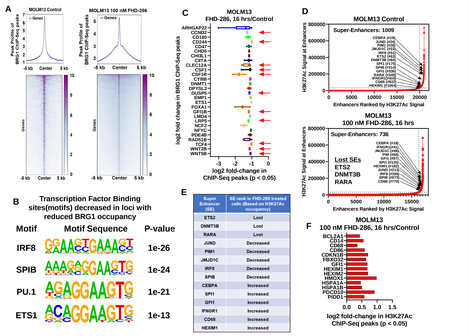

Figure 2. Treatment with FHD-286 depletes BRG1 occupancy on chromatin while increasing H3K27Ac occupancy on loci involved in differentiation and loss of cell viability. A. MOLM13 cells were treated with 100 nM of FHD-286 for 16 hours. ChIP-Seq analysis was conducted with anti-BRG1 antibody. Panel shows the genome wide peak profile and heat map of BRG1 binding at peak center +/- 5 kb resolution. **B.** Transcription Factor binding motifs decreased in loci with reduced BRG1 occupancy. The motif name, canonical binding motif and the p-value are shown. **C.** Log2 fold-decline of BRG1 binding at selected AML relevant loci in MOLM13 treated with 100 nM of FHD-286 for 16 hours. **D-E.** MOLM13 cells were treated with 100 nM of FHD-286 for 16 hours. ChIP-Seq analysis was conducted with anti-H3K27Ac antibody and ranked ordering of super enhancer (ROSE) analysis was performed. **F.** MOLM13 cells were treated with 100 nM of FHD-286 for 16 hours. ChIP-Seq analysis was conducted with anti-H3K27Ac antibody. Panel shows the log2 fold-increase in H3K27Ac occupancy on loci involved in differentiation and loss of viability in MOLM13 cells.

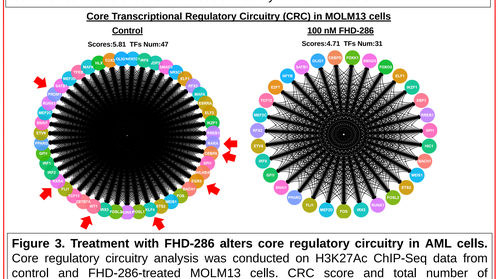

Figure 3. Treatment with FHD-286 alters core regulatory circuitry in AML cells. Core regulatory circuitry analysis was conducted on H3K27Ac ChIP-Seq data from control and FHD-286-treated MOLM13 cells. CRC score and total number of transcription factors in the CRC of untreated and FHD-286-treated cells is shown.

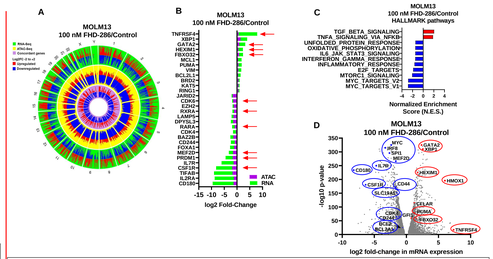

Figure 4. Treatment with FHD-286 concordantly alters chromatin accessibility and mRNA expression in MLL1-rearranged AML cells with reduction in the enrichment scores for MYC, mTORC1, E2F, Interferon-gamma, IL6-JAK-STAT3, as well as of inflammatory response and oxidative phosphorylation gene sets. A-B. MOLM13 cells were treated with 100 nM of FHD-286 for 16 hours as biologic replicates. Bulk nuclei were isolated for ATAC-Seq analysis and total RNA was isolated and utilized for RNA-Seq analysis. RNAs and diffReps-determined ATAC-Seq peaks with ≥ 1.25 fold-change and p <0.05 were utilized for the concordance analysis. Circos plot (**A**) and log2 fold-changes (**B**) of selected, concordant ATAC-Seq and mRNA expression alterations in FHD-286-treated MOLM13 cells. **C**. Gene set enrichment analysis of FHD-286-treated MOLM13 cells compared to HALLMARK pathways. Normalized enrichment scores are shown. All q-values are < 0.1. **D**. Volcano plot of RNA-Seq determined mRNA expression changes in FHD-286-treated MOLM13 cells.

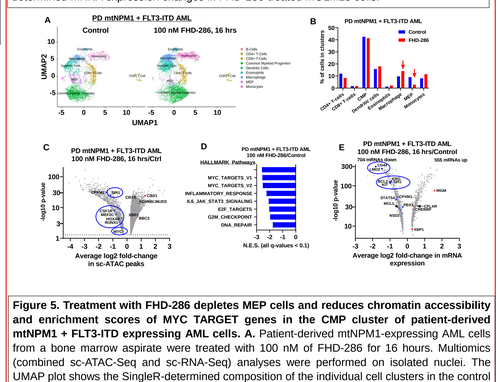

Figure 5. Treatment with FHD-286 depletes MEP cells and reduces chromatin accessibility and enrichment scores of MYC TARGET genes in the CMP cluster of patient-derived mtNPM1 + FLT3-ITD expressing AML cells. A. Patient-derived mtNPM1-expressing AML cells from a bone marrow aspirate were treated with 100 nM of FHD-286 for 16 hours. Multiomics (combined sc-ATAC-Seq and sc-RNA-Seq) analyses were performed on isolated nuclei. The UMAP plot shows the SingleR-determined composition of the individual cell clusters in the control and FHD-286-treated AML cells. **B**. Percentage of each cell type in the clusters of cells from control and FHD-286 treated cells. Arrows indicate clusters with increased or decreased numbers of cells in the FHD-286-treated sample compared to the control sample. **C**. Volcano plot of sc-ATAC-Seq peaks in the CMP cluster with ≥1.25 fold-change up or down and p< 0.05 following treatment with FHD-286. **D**. Gene set enrichment analysis of FHD-286-treated cells over control cells. All q-values are less than 0.1. **E**. Volcano plot of sc-RNA-Seq expression changes (≥1.25 fold-change and p< 0.05) in the CMP cluster following treatment with 100 nM FHD-286 for 16 hours compared to control cells.

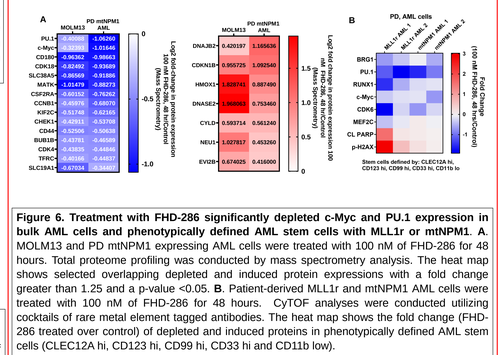

Figure 6. Treatment with FHD-286 significantly depleted c-Myc and PU.1 expression in bulk AML cells and phenotypically defined AML stem cells with MLL1r or mtNPM1. A. MOLM13 and PD mtNPM1 expressing AML cells were treated with 100 nM of FHD-286 for 48 hours. Total proteome profiling was conducted by mass spectrometry analysis. The heat map shows selected overlapping depleted and induced protein expressions with a fold change greater than 1.25 and a p-value <0.05. **B**. Patient-derived MLL1r and mtNPM1 AML cells were treated with 100 nM of FHD-286 for 48 hours. CyTOF analyses were conducted utilizing cocktails of rare metal element tagged antibodies. The heat map shows the fold change (FHD-286 treated over control) of depleted and induced proteins in phenotypically defined AML stem cells (CLEC12A hi, CD123 hi, CD99 hi, CD33 hi and CD11b low).

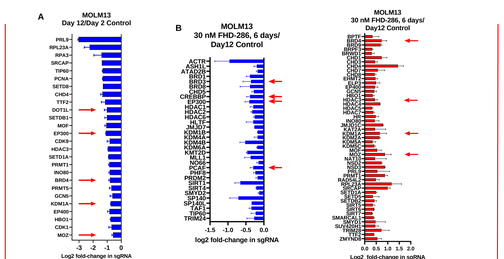

Figure 7. A protein domain-specific CRISPR screen identified druggable co-dependencies and co-enrichments with FHD-286 treatment in MLL1 rearranged AML MOLM13 cells. A. MOLM13 cells expressing Cas9 were transduced with a library of guide RNAs against epigenetic modifier proteins. The panel shows the log2 fold-change (at p <0.05) in guide RNA abundance at 12 days versus 2 days post-transduction. **B**. MOLM13 cells were transduced as in (**A**). Six days post transduction, cells were treated with 30 nM of FHD-286 for 6 days and viable cells were harvested and analyzed for guide RNA abundance. Panels show the log2 fold-change in guide RNAs that were further depleted versus those that were co-enriched by treatment with FHD-286 (p < 0.05). Red arrows indicate druggable dependencies, co-dependencies or co-enrichments.

	Mean Delta Synergy Score		
	FHD-286 + SNDX-50469	FHD-286 + OTX015	FHD-286 + venetoclax
MOLM13	44.47	40.26	17.97
MV4-11	34.90	38.56	48.45
MV4-11 MITR	50.91	55.35	N.D.
OCI-AML3	15.01	25.19	8.16
OCI-AML3 MITR	17.23	8.618	N.D.
PD MLL1-r AML (n=5)	9.20	14.14	11.55
PD mtNPM1 AML (n=4)	11.31	19.53	24.41

	Mean Delta Synergy Score
	FHD-286 + decitabine
MOLM13	42.73
MV4-11	34.28
OCI-AML3	11.99

Figure 8. Co-treatment with FHD-286 and Menin inhibitor SNDX-50469, BET inhibitor OTX015, venetoclax or decitabine induced synergistic *in vitro* lethality in cultured cell lines and patient-derived AML cells expressing MLL-r or mtNPM1 with or without FLT3 alterations. A-B. MOLM13, MV4-11, MV4-11-MITR, OCI-AML3, OCI-AML3-MITR and patient-derived MLL1r or mtNPM1-expressing AML cells were treated with FHD-286 (dose range: 10 nM to 250 nM) and Menin inhibitor SNDX-50469 (dose range: 50 nM to 1000 nM), BET inhibitor OTX015 (dose range: 50 nM to 250 nM) or venetoclax (dose range: 10 nM to 100 nM) or decitabine (dose range: 10 nM to 250 nM) for 72-96 hours. At the end of treatment, the % non-viable cells was determined by staining with TO-PRO-3 iodide and flow cytometry analysis. Delta synergy scores were determined by the ZIP method within the SynergyFinder web application. Synergy scores >1.0 indicate a synergistic interaction of the two agents in the combination. Panel shows the mean Delta Synergy score for each FHD-286-based combination in the cell lines and PD AML cells.

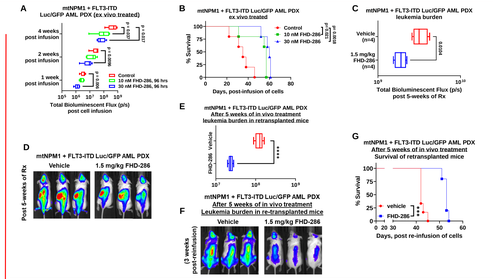

Figure 9. Treatment with FHD-286 exhibits in vivo efficacy against AML initiating stem cells. A. Patient-derived mtNPM1 + FLT3-ITD Luc/GFP cells were ex vivo treated with 10 and 30 nM of FHD-286 for 96 hours. Following this, equal numbers of cells (2.5e6 cells/mouse) were tail vein infused into pre-irradiated (2.5 Gy) NSG mice (n=5 per cohort). The box plots show the total bioluminescent flux (photons/second) at one, two, and four weeks post infusion of the AML cells. **B**. Kaplan-Meier survival curve of NSG mice infused with ex vivo-treated patient-derived mtNPM1 + FLT3-ITD Luc/GFP cells. **C-D**. Patient-derived mtNPM1 + FLT3-ITD Luc/GFP cells were tail vein infused into pre-irradiated NSG mice (n=4 per cohort). Upon engraftment, mice were treated with vehicle or 1.5 mg/kg of FHD-286 for 5 weeks. The box plots show the total bioluminescent flux (photons/second) at five weeks post-infusion of the AML cells. **E**. Viable human AML cells from the spleens and bone marrow of vehicle and FHD-286-treated mice were re-infused into pre-irradiated (2.5 Gy) NSG mice (n=6 per cohort). The box plots show the total bioluminescent flux (photons/second) three weeks post re-infusion of the AML cells. **F**. Representative bioluminescent images of mice from panel E. **G**. Kaplan-Meier survival curve of NSG mice infused with equal numbers of previously in vivo treated PD mtNPM1 + FLT3-ITD Luc/GFP cells.

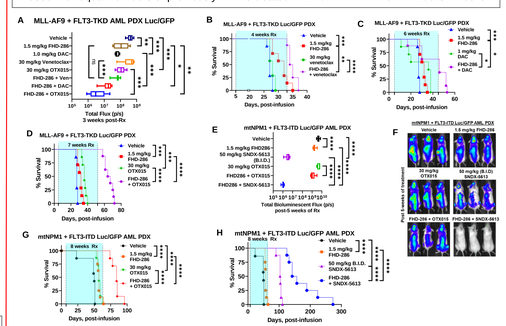

Figure 10. Treatment with FHD-286-based combinations reduced leukemia burden and significantly improved survival of NSG mice bearing MLL-r or mtNPM1-expressing AML xenografts. A. Total photon counts [flux] (determined by bioluminescent imaging) in NSG mice engrafted with luciferized MLL-AF9 + FLT3-TKD AML PDX cells and treated for 3 weeks at the indicated doses. **B-D**. Kaplan-Meier survival plot of NSG mice treated with FHD-286 and venetoclax, DAC, or OTX015. Significance was calculated by a Mantel-Cox log-rank test. **E**. Total photon counts [flux] (determined by bioluminescent imaging) in NSG mice engrafted with luciferized mtNPM1 + FLT3-ITD PDX cells and treated for 3 weeks with FHD-286 and/or SNDX-5613 or OTX015 at the indicated doses. **F**. Representative bioluminescent images of mice from panel (**E**). **G-H**. Kaplan-Meier survival plot of NSG mice engrafted with luciferized mtNPM1 + FLT3-ITD PDX cells and treated with FHD-286 and/or 30 mg/kg of OTX015 or SNDX-5613 for 8 weeks. Significance between cohorts was determined by a Mantel-Cox log-rank test.

Conclusions

1. Treatment with FHD-286 for up to 7 days overcame differentiation block and significantly induced CD11b expression and morphologic features of differentiation in AML cells with MLL-r or mtNPM1 including those with resistance to Menin inhibitor.

2. RNA-Seq analysis of AML cells treated with FHD-286 demonstrated significant reduction in the normalized enrichment scores for expressions of gene-sets of targets of MYC, mTORC1, E2F, Interferon-gamma, IL6-JAK-STAT3, inflammatory response and oxidative phosphorylation genes.

3. Compared to treatment with FHD-286 or venetoclax, decitabine, or OTX015 or vehicle control, co-treatment with FHD-286 and venetoclax, decitabine, or OTX015 exerted superior in vivo anti-AML efficacy without any host toxicity in a PDX model of MLL-r AML.

4. Compared to treatment with FHD-286, OTX015, SNDX-5613 or vehicle control, co-treatment with FHD-286 and OTX015 or SNDX-5613 exerted superior in vivo anti-AML efficacy without host toxicity in a PDX model of mtNPM1 AML.

5. These preclinical findings highlight the promise of FHD-286 treatment alone and in rational combinations in exerting significant anti-AML efficacy against cellular models of AML, especially those with MLL-r or mtNPM1